

1 **Title:** Floating photovoltaics could mitigate climate change impacts on water body temperature and  
2 stratification

3 **Author names and affiliations**

4 Giles Exley<sup>a\*\*</sup>, Alona Armstrong<sup>a,b</sup>, Trevor Page<sup>a</sup>, Ian D. Jones<sup>c</sup>

5 <sup>a</sup>Lancaster Environment Centre, Library Avenue, Lancaster University, Lancaster, LA1 4YQ, UK

6 <sup>b</sup>Energy Lancaster, Science & Technology Building, Lancaster University, Lancaster, LA1 4YF, UK

7 <sup>c</sup>Biological and Environmental Sciences, University of Stirling, Stirling, FK9 4LA, UK

8 \*\*Corresponding author: [g.exley@lancaster.ac.uk](mailto:g.exley@lancaster.ac.uk)

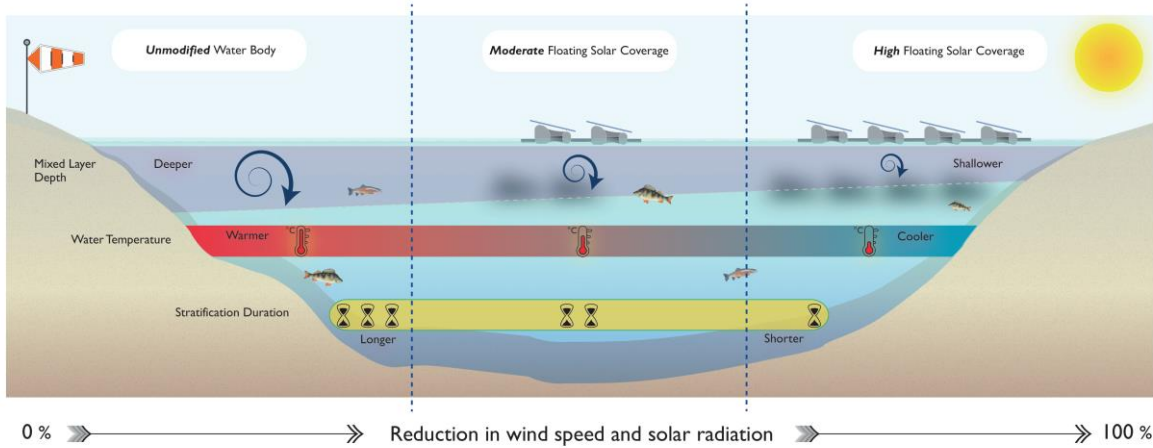
9 **Abstract**

10 Floating solar photovoltaics, or floatovoltaics (FPV), are a relatively new form of renewable energy,  
11 currently experiencing rapid growth in deployment. FPV decarbonises the energy supply while  
12 reducing land-use pressures, offers higher electricity generating efficiencies compared to ground-  
13 based systems and reduces water body evaporation. However, the effects on lake temperature and  
14 stratification of FPV both sheltering the water's surface from the wind and limiting the solar  
15 radiation reaching the water column are unresolved, despite temperature and stratification being  
16 key drivers of the ecosystem response to FPV deployment. These unresolved impacts present a  
17 barrier to further deployment, with water body managers concerned of any deleterious effects. To  
18 overcome this knowledge gap, here the effects of FPV-induced changes in wind speed and solar  
19 radiation on lake thermal structure were modelled utilising the one-dimensional process-based  
20 MyLake model. To resolve the effect of FPV arrays of different sizes and designs, observed wind  
21 speed and solar radiation were scaled using a factorial approach from 0 % to 100 % in 1 % intervals.  
22 The simulations returned a highly non-linear response, dependent on system design and coverage.  
23 The responses could be either positive or negative, and were often highly variable, although, most  
24 commonly, water temperatures reduce, stratification shortens and mixed depths shallow.  
25 Modifications to the thermal dynamics of the water body may subsequently drastically alter  
26 biogeochemical processes, with fundamental implications for ecosystem service provision and water  
27 treatment costs. The extreme nature of response for particular wind speed and solar radiation  
28 combinations results in impacts that could be comparable to, or more significant than, climate  
29 change. As such, depending on how they are used, FPV have the potential to mitigate some of the  
30 impacts of climate change on water bodies and could be a useful tool for water body managers in  
31 dealing with changes to water quality, or, conversely, they could induce deleterious impacts on

32 standing water ecosystems. These simulations provide a starting point to inform the design of future  
33 systems that maximise ecosystem service and environmental co-benefits from this growing water  
34 body change of use.

35 **Keywords:** Floating solar, floatovoltaics, renewables, mixed depth, ecosystem impacts, lake  
36 management

37 **Graphical Abstract**



38

39 **Word Count:** 5453

## 40 1 Introduction

41 Increased energy demands and the urgent need to decarbonise are prompting the rapid deployment  
42 of renewable energy technologies. One such technology, solar photovoltaics (PV), has experienced  
43 exponential growth over the past 25 years (IEA, 2019) and accounted for 57 % of newly installed  
44 renewable energy capacity in 2019 (REN21, 2020). While solar PV has traditionally been ground- or  
45 rooftop-mounted, water-deployed, floating solar photovoltaics (FPV), known colloquially as  
46 floatovoltaics, have emerged in recent years. Global cumulative FPV capacity more than trebled  
47 among the top 70 FPV systems from 2018 to 2019 (Solar Asset Management, 2018; Solarplaza, 2019;  
48 World Bank Group et al., 2019), with a forecasted annual average growth rate of 22 % (Cox, 2019).  
49 Conservative estimates suggest that FPV has a global potential of 400 GW-peak (World Bank Group  
50 et al., 2018), demonstrating the likely widespread uptake of this renewable energy technology.  
51 Although this could be severely hampered by a lack of understanding about the impacts of the  
52 technology on the hosting environment (Gorjian et al., 2021; Lee et al., 2020; Stiubiener et al., 2020;  
53 Zhang et al., 2020; Ziar et al., 2020).

54 FPV systems are typically comprised of five main components: a pontoon of floaters, a mooring  
55 system, PV modules, cabling, and connectors (Sahu et al., 2016). The specific design of a system can  
56 be adapted to suit water body function and application through variations to floater material  
57 (Oliveira-Pinto and Stokkermans, 2020), PV module type (Tina et al., 2021; Ziar et al., 2020),  
58 orientation (Campana et al., 2019), and surface coverage (Cagle et al., 2020). However, each  
59 combination of components will have a unique impact on the atmospheric drivers of lake dynamics,  
60 potentially resulting in a large variation in lake function impacts between systems.

61 A growing body of evidence suggests that FPV has several advantages over conventionally deployed  
62 PV. Firstly, FPV averts the need for large areas of land-use change by occupying the surface of water  
63 bodies (Cagle et al., 2020; Holm, 2017). This is of particular benefit to land-scarce countries and  
64 regions with high land prices (Abid et al., 2019; Campana et al., 2019). Secondly, FPV has been  
65 shown to deliver enhanced performance over ground-based PV due to the cooling effect of the  
66 hosting water body (Choi et al., 2013; Oliveira-Pinto and Stokkermans, 2020; Sacramento et al.,  
67 2015; Yadav et al., 2016). The cooling yield has been found to vary across climates, with heat loss  
68 dependent on wind speed and the openness of the floating structure (Dörenkämper et al., 2021).  
69 Thirdly, and also dependent on system design, FPV has also been shown to reduce evaporative  
70 losses substantially (Choi, 2014; Sahu et al., 2016; Santafe et al., 2014; Taboada et al., 2017),  
71 potentially providing vital water savings for drought-stricken areas. Furthermore, studies have  
72 shown that hydroelectric dams operating in conjunction with FPV can optimise energy efficiency and

73 improve system reliability (Stiubiener et al., 2020; Zhou et al., 2020). Integrated hydroelectric-FPV  
74 systems may also lessen the environmental and social impacts of stand-alone hydroelectric  
75 operation (Sulaeman et al., 2021) providing synergistic benefits to the water-food-energy nexus  
76 (Zhou et al., 2020).

77 Nonetheless, the biological, chemical and physical impacts of FPV on water bodies remain virtually  
78 unknown (Ziar et al., 2020), despite the global importance of water bodies for supplying numerous  
79 ecosystem goods and services (Grizzetti et al., 2019; Maltby et al., 2011; Reynaud and Lanzanova,  
80 2017). Given the forecasted growth in FPV deployment, it is critical that we increase our  
81 understanding of its impact on water bodies. A fundamental starting point to this understanding is  
82 recognising the impacts of FPV on the thermal structure of a water body, as this thermal structure  
83 will be directly affected by FPV and it has a pervasive influence on most other aspects of the  
84 ecosystem (e.g. Diehl et al., 2002; Huisman et al., 2004; Jäger et al., 2008; Macintyre, 1993).

85 A small number of previous studies have considered the effects of natural or artificial floating  
86 elements on lakes (e.g. Maestre-Valero et al., 2013; Ozkundakci et al., 2016). However, their focus  
87 has typically been on specific surface coverage ratios (e.g. Aminzadeh et al., 2018) or particular  
88 ecological effects such as phytoplankton and zooplankton assemblages (e.g. Cazzanelli et al., 2008;  
89 Pinto et al., 2007). Present understanding relating specifically to the ecological impacts of FPV on  
90 lake functioning is limited, with studies typically focussed on technological advancements and  
91 system implementation (e.g. Liu et al., 2017). Of the limited number of studies with an ecological  
92 focus, topics include; the viability of FPV on fish ponds (Chateau et al., 2019); the effect of novel FPV  
93 designs on water quality indicators at an FPV pilot site (Ziar et al., 2020) and the potential impact of  
94 sunlight reduction on biological processes, such as algal blooms (Haas et al., 2020) and  
95 microorganism proliferation in drinking water reservoirs (Mathijssen et al., 2020). Up to now, the  
96 impacts of FPV on water body thermal structure remains unexamined.

97 FPV will both reduce the amount of solar radiation reaching the water and shelter the water from  
98 the effects of wind mixing (Armstrong et al., 2020), modifying water body temperature and  
99 stratification. Wind speed and solar radiation typically have opposite effects on water body thermal  
100 structure. Decreases in wind will tend to increase stratification and surface warming, while  
101 reductions in solar radiation will enhance mixing and cooling of surface water (Kalff, 2002). At  
102 present, it remains unclear whether FPV-induced changes in wind speed or solar radiation will  
103 dominate, as well as the extent of any resulting changes to lake thermal structure. The critical role of  
104 temperature and stratification in determining lake biochemical and ecological processes (Elci, 2008;  
105 Kraemer et al., 2017) means that without this knowledge, deployment of FPV risks inadvertently

106 altering the provisioning of ecosystem goods and services. This could derail future investment in  
107 FPV. Modifications to the processes, function and service delivery of water bodies with an FPV  
108 installation must be carefully managed to ensure the pathway to decarbonisation continues with  
109 minimal concomitant environmental impacts.

110 Here we address this knowledge gap by applying simulations from a one-dimensional, process-based  
111 model and data from a test lake in North West England. We simulate water temperature, mixed  
112 depth and stratification timing to (1) determine the sensitivity of a lake's thermal structure to FPV  
113 deployed at varying scale. We then (2) consider the potential ecosystem consequences and  
114 implications for lake management in a changing climate.

## 115 2 Methods

### 116 2.1 Site description

117 The impacts of FPV on lake thermal structure were modelled for the south basin of Windermere, a  
118 typical monomictic, mesotrophic, deep and temperate lake in the Lake District, North West England.  
119 The south basin of Windermere is long and narrow in shape – with a maximum depth of 42 m, a  
120 mean depth of 16.8 m and a surface area of approximately 6.7 km<sup>2</sup>. As one of the most  
121 comprehensively studied lake systems in the world (Rooney and Jones, 2010), the wealth of  
122 understanding and availability of high-resolution meteorological and in-lake water temperature data  
123 make Windermere an excellent test system for this study (Maberly and Elliott, 2012).

### 124 2.2 Modelling methodology

#### 125 2.2.1 MyLake

126 To resolve the effects of FPV on lake physical properties, we simulated lake variables by adapting an  
127 existing MATLAB model. *MyLake* v1.2 (Saloranta and Andersen, 2007) is a one-dimensional process-  
128 based model, used to simulate the daily vertical distributions of water body temperature,  
129 evaporation and instances of ice cover accurately. *MyLake* partitions horizontal layer volumes by  
130 exploiting interpolated lake bathymetric data, making it similar to other one-dimensional lake  
131 models. The lake water simulation part of the model is based on Ford and Stefan (1980), Riley and  
132 Stefan (1988) and Hondzo and Stefan (1993), while the ice simulation component is based on  
133 Leppäranta (1993) and Saloranta (2000). In brief, the model initially computes the temperature  
134 distribution of the lake for the 24-hour time-step, taking into account diffusive mixing processes and  
135 local heat fluxes. A sequential process then accounts for convective mixing, wind-induced mixing,  
136 the water-ice heat flux and the effect of river inflow (Saloranta and Andersen, 2007). The model has  
137 been successfully applied to various projects as a standalone simulation tool assessing lake

138 thermodynamics and ice regime (e.g. Livingstone and Adrian, 2009; Woolway, R. Iestyn et al., 2017).  
139 Predominantly, model parameters were kept as per the user manual (Saloranta and Andersen,  
140 2004), with minor adjustments made during calibration (see Section 2.4).

### 141 2.2.2 Input data

142 Meteorological data, logged at 4-minute intervals using a Campbell Scientific CR10X data logger,  
143 were obtained from an Automatic Water Quality Monitoring Station (AWQMS) located at the  
144 deepest point of Windermere south basin for 2009. Specifically, air temperature (Skye Instruments  
145 SKH2012) was measured with a relative accuracy of  $\pm 0.35$  °C; relative humidity (HOBO U23-001) with  
146 an accuracy of  $\pm 3$  %; incoming short-wave radiation (Kipp & Zonen CMP6) with a relative accuracy of  
147 5 %, and wind speed (Vector Instruments A100L2) was measured with an accuracy of 1 % for wind  
148 speeds  $> 10.3$  m s<sup>-1</sup> and an accuracy of up to 0.1 m s<sup>-1</sup> for wind speeds  $< 10.3$  m s<sup>-1</sup>. Water  
149 temperature profiles were obtained from 12 stainless-steel sheathed platinum resistance  
150 thermometers (Labfacility PT100), accurate to within 0.1 °C at the following depths; 1, 2, 4, 7, 10, 13,  
151 16, 19, 22, 25, 30 and 35 m. Data were averaged to daily time steps. Estimates for cloud cover (0-1)  
152 were obtained from the R package *insol* (Corripio, 2019), using incoming short-wave radiation data  
153 from the AWQMS. As *MyLake* requires air temperature and relative humidity at 2 m, and wind speed  
154 at 10 m, corrections for measurement height were applied using a modified version of *Lake Heat*  
155 *Flux Analyser* (Woolway et al., 2015b). An iteration scheme with a smoothing function capable of  
156 assessing bulk fluxes at individual time steps allowed the appropriate scheme to be applied for  
157 accurate bulk flux simulation.

158 Daily discharge data from Windermere (River Leven) were used as a proxy for inflow (National River  
159 Flow Archive, 2018), following the assumption that inflow was approximately matched by outflow,  
160 with negligible change in lake level. Lake morphometry (Ramsbottom, 1976) was interpolated to  
161 one-metre intervals. The light attenuation coefficient ( $K_d$ , m<sup>-1</sup>) for Windermere south basin was  
162 obtained from Woolway et al. (2015a).

### 163 2.2.3 Thermal structure simulations

164 The effect on wind speed and solar radiation (forcing variables) for a given percentage coverage of  
165 FPV is unknown and likely to vary substantially depending on the design of the floatovoltaic  
166 deployment. While reductions to both forcing variables are likely, the relative proportions of these  
167 reductions remain to be determined. Here, the forcing variables were altered using a factorial  
168 design, simulating reductions at 1 % intervals from 0 % to 100 %. A factorial design allowed the  
169 identification of non-linear changes and thresholds in the output variables; this was of particular  
170 importance given the range of FPV designs and surface coverages that exist between different

171 systems. Considering reductions to the forcing variables as a whole lake average, not just in the  
172 footprint of the array, maximises transferability between systems with different FPV designs.

### 173 2.3 Data Analysis

174 Mixed layer depth and Schmidt stability were subsequently estimated from modelled water  
175 temperatures using *Lake Analyzer* (Read et al., 2011), a freely available physical limnological tool  
176 (e.g. Kraemer et al., 2015; Read et al., 2012). Mixed layer depth was estimated using the  
177 metalimnion extent function, an algorithm that defines the approximate depth of the base of the  
178 mixed layer using a density gradient threshold of  $0.1 \text{ kg m}^{-3} \text{ m}^{-1}$ . Mean mixed layer depth for the  
179 stratified period of each scenario, along with annual mean mixed layer depth were calculated.

180 The onset of thermal stratification was defined from the depth-resolved temperature simulations as  
181 the time when the temperature differential between the surface (0 m) and the bottom (42 m) of the  
182 lake exceeded  $1 \text{ }^\circ\text{C}$  (Fee et al., 1996). Alterations to stratification duration were assessed by  
183 calculating the longest stratified period, defined here as the greatest number of consecutive days of  
184 stratification across the simulated period. This was then compared to the stratified period of the  
185 water body without FPV (unmodified system), permitting the calculation of a gain or loss in stratified  
186 days. Stratification onset and overturn days were derived from these data, with onset being the first  
187 day and overturn being the final day of the longest stratified period.

188 Three simulation scenarios were considered in further detail. The first being an equal (1:1) reduction  
189 to each forcing variable. Given the relative proportions of reductions to forcing variables remain  
190 unknown and are likely to vary substantially depending on FPV design (see Section 2.2.3), two  
191 scenarios with scaled forcing variables were simulated. A 'wind dominant' scenario where the wind  
192 speed reduction scales as 80 % of the solar radiation reduction and a 'solar dominant' scenario  
193 where the reduction to solar radiation scales as 80 % of the wind speed reduction.

### 194 2.4 Model Calibration

195 The model was calibrated for a one-year period against observed water body temperatures.  
196 Standard calibration procedures were undertaken following Moriasi et al. (2007). Briefly, calibration  
197 of the scaling of forcing variables was guided by Monte Carlo sampling of uniform parameter  
198 distributions. The Nash-Sutcliffe model efficiency coefficient (NSE) (Nash and Sutcliffe, 1970) and the  
199 Root Mean Square Error (RMSE) for metalimnion top, Schmidt stability and volume average  
200 temperature (see supplementary information) were used to identify the best simulation. Slight  
201 modifications to scale the original driving data were required to achieve the optimum parameter  
202 values for the calibration year; these were +2 % for wind speed and +13 % for solar radiation. These  
203 modifications are within the instrumentation error range and help reflect the variation likely

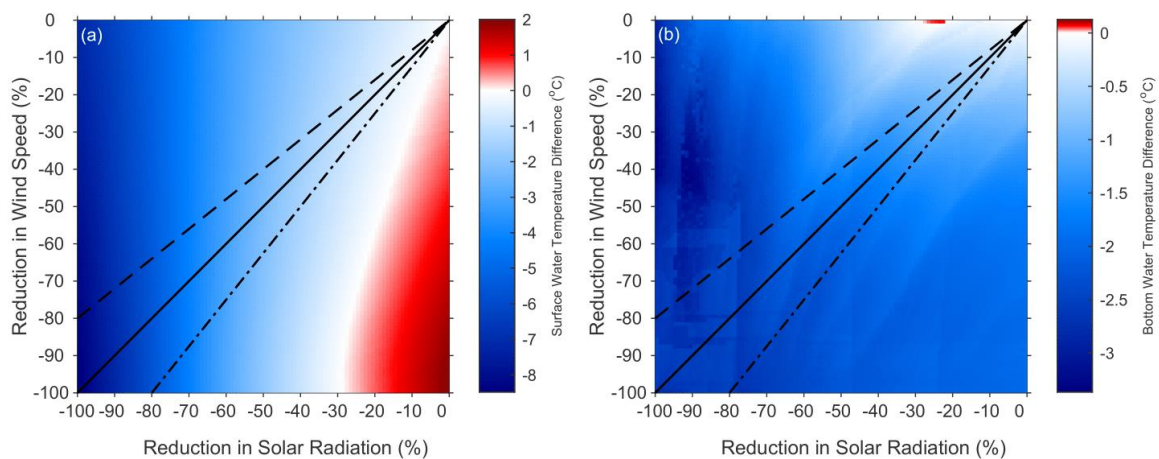
204 experienced in forcing variables across the whole of the water body. Thus, driving the model using  
205 2009 measured meteorological data with a wind speed multiplier of 1.02 and a solar radiation  
206 multiplier of 1.13 provided the optimum fit against the observed in-lake temperature data and this  
207 then constituted the baseline model simulation.

### 208 3 Results

209 After calibration, simulated water temperatures, volume averaged temperatures, mixed layer depth  
210 and Schmidt stability compared favourably to the observed data (Figure S1). Model efficiency  
211 computed with NSE ranged from 0.93 to 0.97, an encouraging indication of the ability of the model  
212 to reproduce the system response (see supplementary information for full calibration details, Table  
213 S1).

#### 214 3.1 Response of water body temperature to FPV

215 Modelled reductions to the forcing variables generally reduced annual mean surface water  
216 temperatures (Figure 1a). Surface water temperature reductions were non-linear, with small  
217 reductions to the forcing variables having a negligible effect and larger reductions having an  
218 increasingly greater effect (Table S2). Increases in surface water temperatures occurred only in  
219 scenarios when wind speed was reduced considerably more than solar radiation. Similarly, annual  
220 mean bottom temperatures generally decreased, albeit less than surface temperatures (Figure 1b).  
221 As could be expected, given the reductions in surface and bottom water temperatures, mean annual  
222 volume average temperature was reduced for all scenarios (Figure S2).

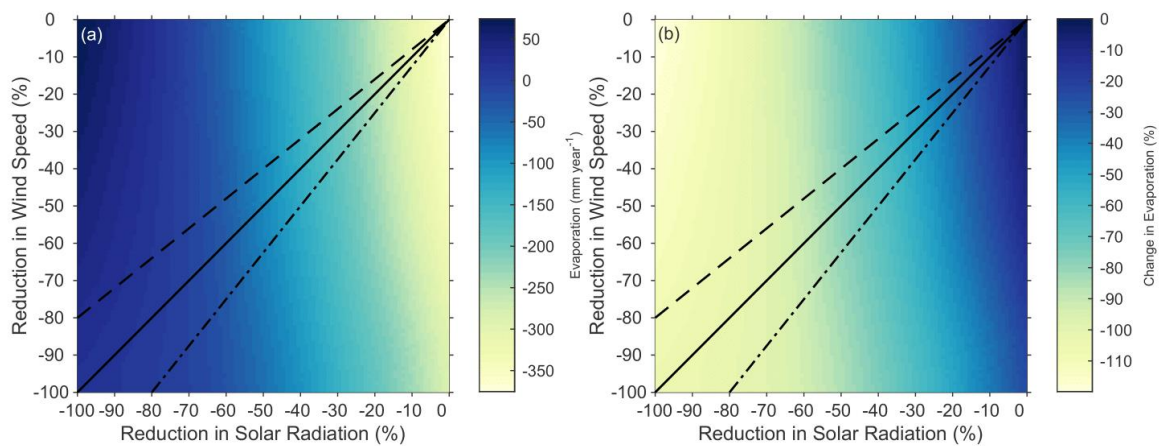


223  
224 *Figure 1 - Differences in mean surface and bottom water temperatures. Results are shown for mean annual (a) surface*  
225 *water temperature and (b) bottom water temperature. Water temperatures for the unmodified system were (a) 11.2 °C and*  
226 *(b) 7.0 °C. The solid black line represents an equal wind speed and solar radiation reduction approximating floating solar*  
227 *coverage (1:1). A wind dominant scenario (solar radiation reduced more than wind speed) is shown with a dashed line. The*  
228 *dot-dash line represents a solar dominant scenario (wind speed reduced more than solar radiation).*



229 In 2009 there was no ice-cover on the lake and, indeed, ice cover on Windermere is very rare.  
 230 Nevertheless, simulations with more than a 90 % reduction to the forcing variables resulted in  
 231 sufficiently cold surface water temperatures for ice to form (Figure S3). Ice cover duration increased  
 232 as the forcing variables were further reduced above 90 %. For example, a 90 % 1:1 reduction  
 233 resulted in 22 days of ice cover, while a 98 % reduction resulted in 43 days of ice cover.

234 Each reduction to the forcing variables decreased total annual evaporation in comparison to the  
 235 baseline (Figure 2). At a 74 % 1:1 forcing variable reduction, a threshold was crossed where dew  
 236 formed on the lake surface, providing an annual net gain in water. Wind dominant scenarios (solar  
 237 reduced by more than wind) saw greater reductions in evaporation than in solar dominant scenarios  
 238 (Table S2).



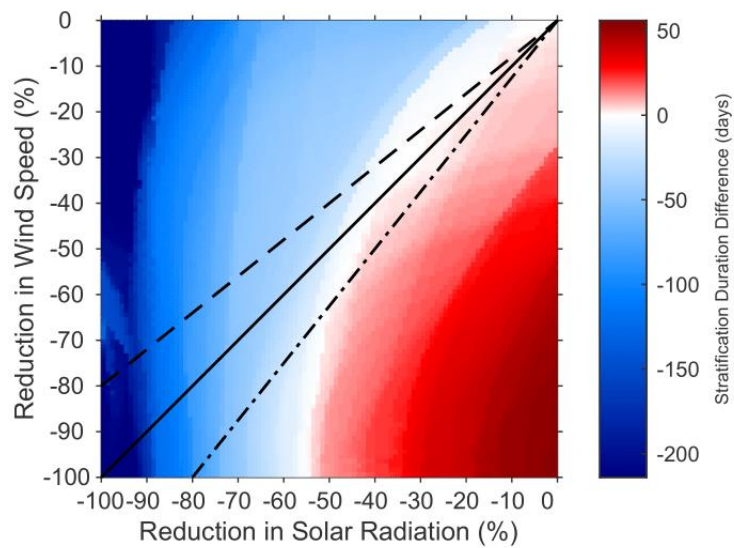
239  
 240 *Figure 2 - Annual evaporation and change in evaporation. Results are shown for (a) total annual evaporation. A negative*  
 241 *value indicates a net loss of water from the lake, while a positive value indicates a net gain in water. (b) The percentage*  
 242 *change in evaporation in comparison to the baseline (375.2 mm year<sup>-1</sup>). The solid black line represents an equal wind speed*  
 243 *and solar radiation reduction approximating floating solar coverage (1:1). A wind dominant scenario (solar radiation*  
 244 *reduced more than wind speed) is shown with a dashed line. The dot-dash line represents a solar dominant scenario (wind*  
 245 *speed reduced more than solar radiation).*

## 246 3.2 Response of stratification duration and strength to FPV

### 247 3.2.1 Stratification duration

248 When reductions to the forcing variables were 1:1 and did not exceed 45 %, stratification duration  
 249 was similar ( $\pm$  three days) to that of Windermere without FPV (Figure 3). Reductions in excess of this  
 250 threshold decreased stratification duration by  $\sim$ 39 days for every additional 10 % reduction to the  
 251 forcing variables (Table S3a). However, when the reductions to the forcing variables were not 1:1,  
 252 stratification duration was modified even with small reductions. A solar dominant scenario, for  
 253 example, increased stratification duration for all scenarios up to a 52 % solar reduction, ranging from  
 254 3 to 13 days increase. The opposite was true when wind dominated, with stratification duration

255 decreasing for all scenarios by a minimum of 29 days, up to a maximum of 214 days. Solar radiation  
256 reductions tended to dominate over wind speed reductions in determining stratification duration.

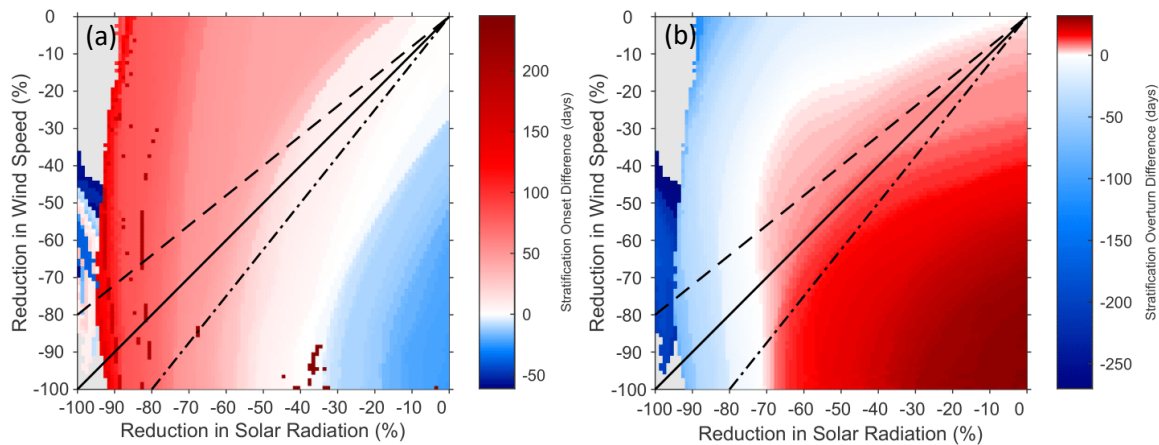


257

258 *Figure 3 - Stratification duration for each scenario. The unmodified system was stratified for 214 days. The solid black line*  
259 *represents an equal wind speed and solar radiation reduction approximating floating solar coverage (1:1). A wind dominant*  
260 *scenario (solar radiation reduced more than wind speed) is shown with a dashed line. The dot-dash line represents a solar*  
261 *dominant scenario (wind speed reduced more than solar radiation).*

### 262 3.2.2 Stratification Onset & Overturn

263 FPV deployment shifted the stratified period to later in the year, with delayed onset and overturn  
264 (Table S3a, b). Wind dominant scenarios typically delayed stratification, where wind speeds  
265 remained proportionally higher than solar radiation (dashed-line Figure 4a). However, in scenarios  
266 where the wind speed was reduced by at least 30 %, but solar radiation remained little changed,  
267 onset occurred earlier in the year. Overturn was delayed by up to 10 days as a consequence of  
268 reduced wind speed when 1:1 forcing variable reductions were less than 72 %. Above 72 %, the  
269 dominant forcing variable switched, with reduced solar radiation advancing overturn timing  
270 (Figure 4b).



271

272 *Figure 4 - Stratification onset and overturn. Change in day of year shown for (a) onset and (b) overturn of thermal*  
 273 *stratification with modified wind speed and solar radiation. A negative value indicates an earlier day of the year*  
 274 *(advancement), while a positive value indicates a later day of the year (postponement). Stratification onset and overturn*  
 275 *occurred at day 102 and 315 respectively. The solid black line represents an equal wind speed and solar radiation*  
 276 *approximating floating solar coverage (1:1). A wind dominant scenario (solar radiation reduced more than wind speed) is*  
 277 *shown with a dashed line. The dot-dash line represents a solar dominant scenario (wind speed reduced more than solar*  
 278 *radiation).*

### 279 3.2.3 Stability

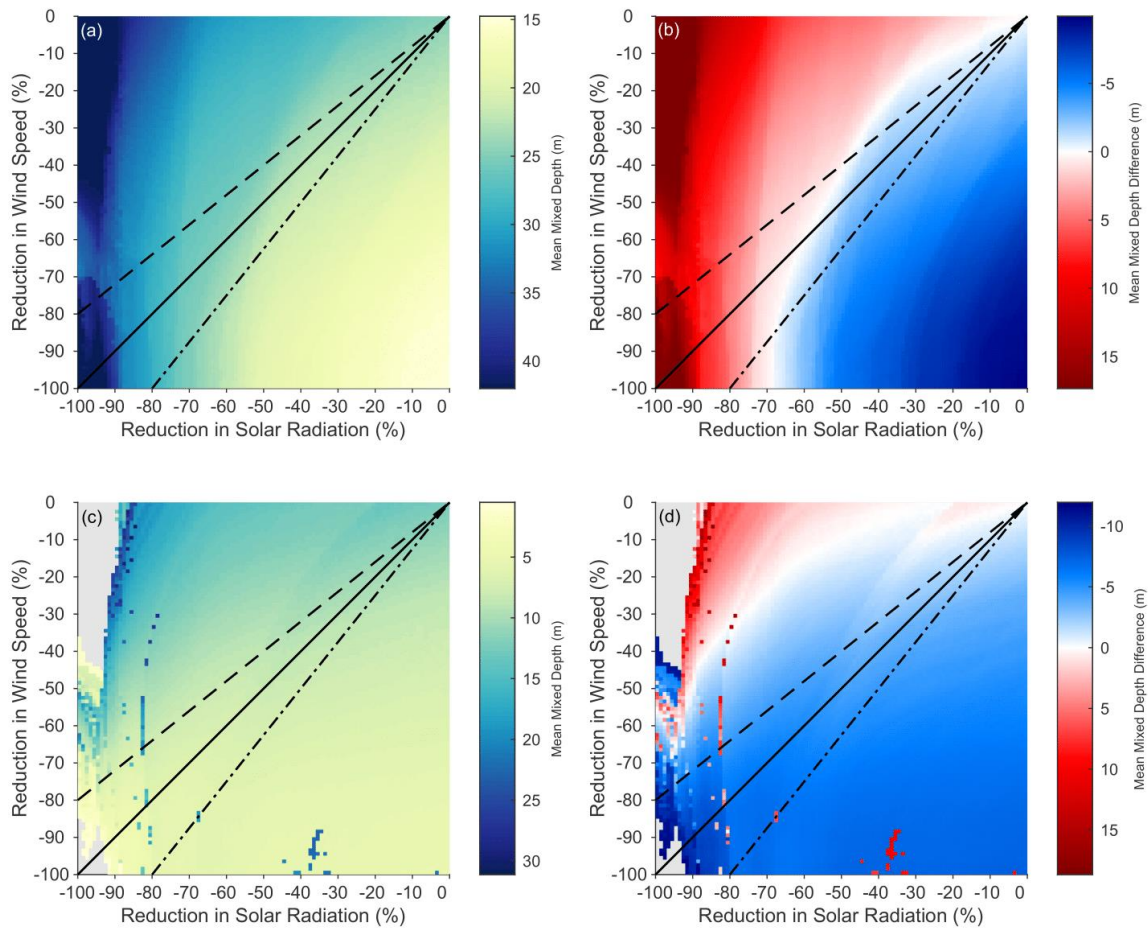
280 Forcing variable reductions of up to 13 % modified Schmidt stability by a relatively modest  $\pm 10 \text{ J m}^{-2}$ ,  
 281 within 3 % of the unmodified system. Scenarios where FPV reduced forcing variables by more than  
 282 13 % reduced Schmidt stability substantially (Figure S4). The stability of the water body only  
 283 increased in instances when wind speed was reduced considerably, with solar radiation reduced by  
 284 no more than 20 %. A 10 % solar radiation reduction and a 50 % wind speed reduction, for example,  
 285 increased mean annual Schmidt stability by  $59 \text{ J m}^{-2}$ . When each forcing variable was reduced by  
 286 50 %, Schmidt stability was reduced by  $126 \text{ J m}^{-2}$ . Solar radiation changes were generally the  
 287 dominant factor determining Schmidt stability, seen by the vertical bands in Figure S4; changing the  
 288 wind speed had less influence, especially at higher reductions of solar radiation.

### 289 3.3 Mixed Depth

290 Annual mean mixed depth shallowed with 1:1 forcing variable reductions of up to 60 % (1:1)  
 291 (Table S4a), indicated by the negative mixed depth difference. Reductions greater than 60 % (1:1)  
 292 deepened the annual mean mixed depth, with the water body remaining mixed all year when  
 293 reductions exceeded 94 % (1:1) (Figure 5a, b). Mixed depth was shallowed by 0.58 m for every 10 %  
 294 reduction to the forcing variables up to 40 % (1:1).

295 These changes in annual mixed depth were, in part, caused by the changes in stratification duration.  
 296 Excluding this effect by focussing only on the stratified period, each scenario demonstrated a

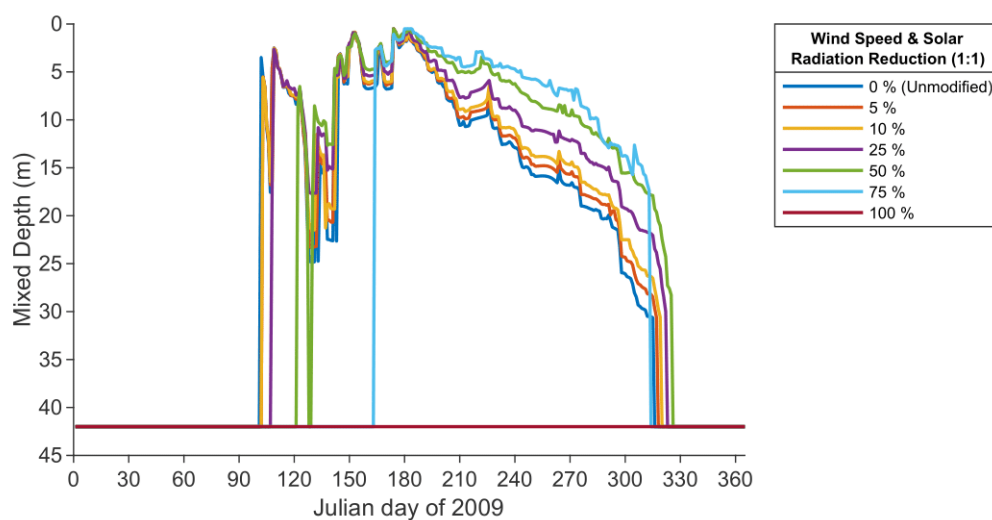
297 shallowing of mean summertime mixed depth for all 1:1 reductions (Figure 5c, d). Reductions in  
 298 excess of 81 % were highly non-linear (1:1), while smaller reductions were relatively proportional to  
 299 the forcing variable reduction. The effect of FPV on mixed depth was considerable, with 85 % of all  
 300 scenarios shallowing for the stratified period (Table S4b). Net summertime deepening occurred for  
 301 the remaining scenarios, typically when very large changes to solar radiation were coupled with only  
 302 small changes to wind speed. Mixed depth was at least halved for 29 % of all scenarios.



303  
 304 *Figure 5 - Annual and stratified period mixed depths for each scenario. Results shown for (a) annual mean mixed depth, (b)*  
 305 *difference from the baseline for annual mean mixed depth, (c) mean mixed depth for the stratified period and (d) the*  
 306 *difference in mean mixed depth for the stratified period of each scenario with modified wind speed and solar radiation. A*  
 307 *negative value on (b) or (d) indicates mixed depth has shallowed, i.e. has moved closer to the surface of the water body. A*  
 308 *positive value on (b) or (d) indicates a deepening of mixed depth, i.e. mixed depth has shifted towards the bottom of the*  
 309 *water body. Annual and stratified period mean mixed layer depth were 24.7 m and 12.4 m, respectively. The solid black line*  
 310 *represents an equal wind speed and solar radiation reduction approximating floating solar coverage (1:1). A wind dominant*  
 311 *scenario (solar radiation reduced more than wind speed) is shown with a dashed line. The dot-dash line represents a solar*  
 312 *dominant scenario (wind speed reduced more than solar radiation).*

313 There were strong seasonal dynamics in mixed depth, with progressive deepening throughout the  
 314 summer months for scenarios where forcing variables were reduced by up to 75 % (1:1) (Table S5;

315 Figure 6). Daily mixed depths, for scenarios with forcing variable reductions of 5, 10, 25, 50 and 75 %  
 316 (1:1) were initially closely aligned to the mixed layer depth of the unmodified system (Figure 6). At  
 317 day 175 (24/06/09) the mixed depth of each scenario diverged from the unmodified system before  
 318 converging again at day 325 (21/11/09). During the diverged period, scenarios with forcing variable  
 319 reductions of 10 % or greater differed substantially from the unmodified system, with mean mixed  
 320 depths differing by more than 2 m. Although the trend remained consistent, the magnitude did vary.  
 321 The difference in mixed depth peaked at 15.4 m for the 75 % scenario on day 305 (01/11/09). A  
 322 100 % (1:1) reduction to the forcing variables kept the water body fully mixed throughout the  
 323 entire year.



324  
 325 *Figure 6 - Daily mixed depth. The scenarios shown have equal wind speed and solar radiation reductions approximating*  
 326 *floating solar coverage (1:1).*

## 327 4 Discussion

328 Lake thermal structure is dependent on a range of factors, including weather conditions, lake  
 329 morphology and geographical location (Kalff, 2002). Although FPV deployments will alter net wind  
 330 speed and solar radiation at the lake surface, the simulations here did not assume a specific extent  
 331 of coverage or system design. Instead, we considered the effects of varying the scale of the forcing  
 332 variables. For this discussion, we use only the assumption that surface coverage is negatively  
 333 correlated with the forcing variables, i.e. that higher surface coverages cause a greater reduction in  
 334 wind speed and solar radiation.

335 Thermal responses to differing reductions in wind speed and solar radiation varied enormously, from  
 336 the negligible to the very large. Proportionate increases in alteration of driving forces resulted in  
 337 highly non-linear responses. Both positive and negative responses were possible, depending on the

338 changes to the driving variables, reflecting the opposite effects that wind speed and solar radiation  
339 typically have on lake thermal structure. The responses most commonly seen, though, were for  
340 temperatures to reduce, stratification to shorten, but mixed depths to become shallower. In the  
341 small number of instances when water temperature increased or stratification duration lengthened,  
342 an FPV system would need to cause substantial wind speed reductions and minimal solar radiation  
343 reductions. Conversely, the rare instance of mixed depth deepening (when considered during the  
344 stratified period only) occurred when substantial solar radiation reductions were coupled with  
345 minimal wind speed reductions.

## 346 4.1 The sensitivity of lake thermal structure to FPV

### 347 4.1.1 Cooling effect on water temperature

348 Water temperature changes were minor for small coverages of FPV, while more extensive FPV  
349 coverages drove major decreases (Figure 1). As many metabolic processes are highly temperature-  
350 dependent, the deployment of FPV at large coverages has the potential to change the functioning of  
351 lentic ecosystems by modifying animal behaviour, food web dynamics, life histories, species  
352 interactions and carbon cycling (Kraemer et al., 2017; Tranvik et al., 2009). Reduced water  
353 temperatures may also present operational challenges, particularly to networks comprised of cast  
354 iron distribution mains. During the colder winter months, increased tensile stresses from reduced  
355 water temperatures may lead to pipe fractures and an increased incidence of pipe  
356 bursts (Jesson et al., 2010).

357 Cooler water temperatures and greatly reduced wind speeds permitted the formation of ice at high  
358 surface coverages (Figure S3), shifting the lake from a monomictic to a dimictic stratification regime.  
359 This considerable temporal shift in ice cover regime may have implications for cyanobacterial  
360 community composition (Ozkundakci et al., 2016) and fish behaviour (Jurvelius and Marjomki, 2008)  
361 while enhancing cultural ecosystem service provisioning (Knoll et al., 2019). In water bodies where  
362 FPV deployment could induce ice-cover, consideration would need to be given in the FPV design to  
363 mitigate the possibilities of compression forces and the restriction of array movement due to  
364 ice cover.

### 365 4.1.2 Changes to stratification length

366 Typically, the interception of incoming solar radiation by FPV extended the period of water column  
367 heating required in the spring before a density gradient established, postponing thermal  
368 stratification onset (Figure 4). Delayed epilimnion formation has been shown to shift the timing of  
369 spring phytoplankton blooms to later in the year (Meis et al., 2009), a phenological

370 desynchronization which could lead to trophic mismatch, affecting the wider food web hierarchy  
371 (Thackeray et al., 2013; Visser and Both, 2005).

372 At low to moderate FPV coverages, stratification duration increased a little, and more so when wind  
373 reductions were substantially greater than solar radiation reductions (Figure 3), increasing the  
374 likelihood of hypolimnetic anoxia and the increased regeneration of soluble phosphorus and metals  
375 from the lake sediment (Beutel et al., 2008; Forsberg, 1989). The regeneration of heavy metals from  
376 lakebed sediment degrades water quality, necessitating enhanced water treatment, although the  
377 postponement of overturn may mean extra nutrient releases occur at periods of lower light  
378 availability when conditions are less suitable for phytoplankton growth (Butcher et al., 2015). At  
379 higher FPV coverages and scenarios with enhanced solar reduction, stratification duration  
380 shortened, which would tend to have the opposite effect of reducing anoxia and internal loading of  
381 nutrients and metals. The possibility of either outcome, increase or decrease, for such critical  
382 components of water quality emphasises the need for astute system design.

#### 383 4.1.3 Alteration of mixed layer depth

384 While it was more common in the model results that water temperature was lowered, stability  
385 reduced and stratification shortened, mixed layers typically were shallowed, not deepened  
386 (Figure 5). Thus, reductions in solar radiation seemed to be more influential than wind speed  
387 reductions on water temperature and stratification, but the reduction in wind speed more influential  
388 on the depth of the epilimnion. As a fundamental driver of the chemistry and biology of lake  
389 ecosystems, the modification of mixed layer depth by FPV is of considerable importance for water  
390 quality (Kraemer et al., 2015; North et al., 2014; Yankova et al., 2017). FPV deployments will reduce  
391 photosynthetically active radiation (PAR) directly under array structures as well as mixed depth, so  
392 the ratio of epilimnetic depth to euphotic depth will alter, impacting phytoplankton growth  
393 (Huisman et al., 1999). Individual phytoplankton species with adaptations well suited to the modified  
394 epilimnetic depth to euphotic depth ratio beneath an FPV array will thrive, so changes in biomass  
395 and species composition should be expected. Non-continuous FPV deployments that allow a mosaic  
396 of light availability will complicate alterations to the phytoplankton community further. In particular,  
397 and of concern for water body managers, toxic cyanobacteria are well adapted to such conditions,  
398 utilising gas vesicles to regulate their buoyancy (Walsby et al., 1997). Simulations by Haas et al.  
399 (2020) found FPV systems that reduced light attenuation by 40 %, or more, greatly reduced algal  
400 biomass, although they did not consider the effects of reduced wind speed, which may improve  
401 conditions for phytoplankton growth. The use of semi-transparent PV modules which provide  
402 specific transmittance windows to control light intensities have been proposed as a means to  
403 regulate phytoplankton growth (Zhang et al., 2020).

## 404 4.2 FPV and lake management in the context of a changing climate

405 The deployment of FPV is a direct response to the need to decarbonise the global energy supply in  
406 order to avert catastrophic climate change. Simulations here demonstrate that the effects on lake  
407 thermal structure of certain combinations of forcing variable reduction can be as, or more  
408 influential, than effects induced by climate change, and could either mitigate or exacerbate the  
409 impact. Numerous studies have identified increasing lake temperatures due to climate change,  
410 which are predicted to disturb both ecological and biogeochemical processes (e.g. O'Neil et al., 2012;  
411 Paerl and Paul, 2012; Thackeray et al., 2008). Woolway et al. (2019) found the average annual  
412 minimum surface-warming rate of eight lakes to be  $0.35\text{ }^{\circ}\text{C decade}^{-1}$ , while O'Reilly et al. (2015)  
413 found 235 globally distributed lakes' summer surface water temperatures were warming at a mean  
414 trend of  $0.34\text{ }^{\circ}\text{C decade}^{-1}$ . Thus, FPV may provide a useful tool for water body managers in mitigating  
415 against lake warming. For example, a decade of lake surface temperature warming could be  
416 mitigated with the deployment of an FPV array at a surface coverage that reduces lake-average wind  
417 speed and solar radiation by approximately 10 % (Figure 1).

418 A further example of climate change mitigation, and of particular relevance to water-scarce  
419 locations, is the reduction in evaporation achieved by increasing FPV coverage (Figure 2). Cooler  
420 surface water temperatures weaken the water-to-air vapour pressure difference (Oke, 2002) while  
421 the FPV array intercepts incoming radiative energy, reducing the latent heat flux (Aminzadeh et al.,  
422 2018). Although research has previously identified that FPV will reduce evaporative losses (e.g.  
423 Ferrer-Gisbert et al., 2013; Redón-Santafé et al., 2014; Taboada et al., 2017), here it is also shown  
424 that the cooler surface water under FPV relative to the warmer, moist air above the water body  
425 permits dew deposition (Oke, 2002). At coverages greater than 74 % (1:1 forcing variable reduction)  
426 a tipping point is crossed, resulting in a net gain of water to the lake.

427 However, while FPV could be an effective tool to mitigate against lake warming, FPV facilitated  
428 prolonged stratification duration and delayed overturn for some scenarios simulated in this study,  
429 with the potential consequences similar to those of climate warming (e.g. Adrian et al., 1995;  
430 Woolway and Merchant, 2019). Foley et al. (2012) examined long-term changes in stratification  
431 dynamics for a lake close to Windermere between 1968 and 2008; they found climate warming led  
432 to onset occurring 28 days earlier, overturn 18 days later, and the duration of stratification increased  
433 by 38 days. While FPV may be able to lessen the earlier onset of stratification brought about by  
434 climate change, the simulations show FPV deployment at lower coverages may also exacerbate the  
435 effects of climate change, potentially lengthening stratification duration and postponing  
436 overturn further.



### 437 4.3 FPV deployment best practice

438 These simulations show impacts on water body process and function in response to the deployment  
439 of FPV, with results which are relevant for other monomictic and mesotrophic deep lakes in the  
440 temperate zone, although variations in local climate may constrain or exacerbate many of the  
441 effects identified in this study. Any wider extrapolation of these impacts needs to take into  
442 consideration geographical and morphological factors that affect lake-atmosphere interactions. For  
443 example, ice cover, which occurred with high FPV coverage rates, would not occur in tropical regions  
444 due to higher air temperatures. Lakes in tropical regions also undergo different mixing regimes and  
445 tend to have less vertical temperature difference than temperate lakes (Lewis, 1987), so may  
446 respond differently to a temperate system. As latitude also influences turbulent surface heat fluxes  
447 (Woolway et al., 2018) and atmospheric stability above lakes (Woolway, et al., 2017), geographical  
448 location is likely to be a key contributor to the overall effect of FPV on lake thermal structure. The  
449 response of lakes with differing morphometric characteristics must also be considered; lake surface  
450 area, volume and mean depth are pertinent drivers of lake thermal structure (Kraemer et al., 2015;  
451 Lerman et al., 1995; Talling, 2001; Wetzel, 2001). In smaller lakes, convection is the dominant driver  
452 of mixed-layer turbulence, while wind shear is the primary driver for larger lakes (Read et al., 2012).  
453 Lakes of a smaller surface area have broader diel temperature ranges than larger lake-systems  
454 making them more prone to disturbance (Woolway et al., 2016). The temporal variation in these  
455 drivers will further modify the response between individual systems.

456 The number of water bodies hosting FPV arrays will increase with the sustained global drive to  
457 decarbonise energy supplies; therefore, we anticipate an urgent need for further understanding on  
458 the effects of FPV. Critically the model simulations demonstrate a high sensitivity to extent and  
459 design of deployments with highly non-linear thermal responses and both increases or decreases in  
460 temperature and stratification being possible. The model simulations suggest only a few percent  
461 cover (< 10 %) of FPV typically only induces minor changes, but more significant covers (> ~50 %)   
462 result in large temperature changes and very extensive modifications to stratification timing. The  
463 effects of FPV at larger coverages are of a similar magnitude to that of climate change. This  
464 considerable variation in possible response provides those deploying FPVs an opportunity to utilise  
465 deployments for actively enhancing water quality benefits as well as decarbonising electricity  
466 production.

## 467 5 Conclusion

468 By simulating the response of a lake to FPV deployed at varying extent, this study has demonstrated  
469 patterns of increased impact with increased perturbation, ranging from negligible to very large.

470 Based on these findings, future FPV designs should consider the following to maximise ecosystem  
471 co-benefits and limit potential harm:

- 472 • Reductions in wind speed and solar radiation as an average across the lake cause a non-  
473 linear, complex response with the direction of these effects dependent on FPV array design,  
474 including coverage density
- 475 • Low FPV surface coverages had a negligible effect on the thermal structure of the test  
476 system, while high coverages were a major disruptor of the archetypal thermal structure
- 477 • FPV deployments may have impacts that are as, or more, influential than catastrophic  
478 climate change, therefore providing an opportunity to manage the effects of climate change  
479 on lake systems actively
- 480 • Appropriate design and deployment of FPV will be required to mitigate the likelihood of  
481 hypolimnetic anoxia and to optimise changes in the composition of phytoplankton  
482 communities as FPV modifies lake thermal structure and light climate

483 FPV is a substantial perturbation to water body process and function. Deployment with minor  
484 impact is possible, but the infancy of knowledge on FPV necessitates planning and impact  
485 assessment on a system-by-system basis.

486

487 **Declaration of competing interest**

488 The authors declare that they have no known competing financial interests or personal relationships  
489 that could have appeared to influence the work reported in this paper.

490 **Acknowledgements**

491 Funding: This work was supported by the Natural Environment Research Council (grant number  
492 NE/R010226/1) and United Utilities, with GE's Industrial CASE studentship through the Envision  
493 Doctoral Training Partnership. AA was supported by a NERC Industrial Innovation Fellowship (grant  
494 number: NE/R013489/1).

## 495 6 References

496

497 Abid, M., Abid, Z., Sagin, J., Murtaza, R., Sarbassov, D., Shabbir, M., 2019. Prospects of floating  
498 photovoltaic technology and its implementation in Central and South Asian Countries. *International*  
499 *Journal of Environmental Science and Technology* 16(3), 1755-1762.

500

501 Adrian, R., Deneke, R., Mischke, U., Stellmacher, R., Lederer, P., 1995. A long-term study of the  
502 Heiligensee (1975-1992). Evidence for effects of climatic change on the dynamics of eutrophied lake  
503 ecosystems. *Archiv für Hydrobiologie* 133(3), 315-337.

504

505 Aminzadeh, M., Lehmann, P., Or, D., 2018. Evaporation suppression and energy balance of water  
506 reservoirs covered with self-assembling floating elements. *Hydrol Earth Syst Sc* 22(7), 4015-4032.

507

508 Armstrong, A., Page, T., Thackeray, S.J., Hernandez, R.R., Jones, I.D., 2020. Integrating environmental  
509 understanding into freshwater floatovoltaic deployment using an effects hierarchy and decision  
510 trees. *Environmental Research Letters* 15(11).

511

512 Beutel, M.W., Leonard, T.M., Dent, S.R., Moore, B.C., 2008. Effects of aerobic and anaerobic  
513 conditions on P, N, Fe, Mn, and Hg accumulation in waters overlaying profundal sediments of an  
514 oligo-mesotrophic lake. *Water Res* 42(8-9), 1953-1962.

515

516 Butcher, J.B., Nover, D., Johnson, T.E., Clark, C.M., 2015. Sensitivity of lake thermal and mixing  
517 dynamics to climate change. *Climatic Change* 129(1-2), 295-305.

518

519 Cagle, A.E., Armstrong, A., Exley, G., Grodsky, S.M., Macknick, J., Sherwin, J., Hernandez, R.R., 2020.  
520 The Land Sparing, Water Surface Use Efficiency, and Water Surface Transformation of Floating  
521 Photovoltaic Solar Energy Installations. *Sustainability* 12(19).

522

523 Campana, P.E., Washhage, L., Nookuea, W., Tan, Y.T., Yan, J.Y., 2019. Optimization and assessment of  
524 floating and floating-tracking PV systems integrated in on- and off-grid hybrid energy systems. *Solar*  
525 *Energy* 177, 782-795.

526

527 Cazzanelli, M., Warming, T.P., Christoffersen, K.S., 2008. Emergent and floating-leaved macrophytes  
528 as refuge for zooplankton in a eutrophic temperate lake without submerged vegetation.  
529 *Hydrobiologia* 605, 113-122.

530

531 Chateau, P.A., Wunderlich, R.F., Wang, T.W., Lai, H.T., Chen, C.C., Chang, F.J., 2019. Mathematical  
532 modeling suggests high potential for the deployment of floating photovoltaic on fish ponds. *Sci Total*  
533 *Environ* 687, 654-666.

534

535 Choi, Y.-K., 2014. A study on power generation analysis of floating PV system considering  
536 environmental impact. Republic of Korea.

537

538 Choi, Y.-K., Lee, N.-H., Kim, K.-J., 2013. Empirical Research on the efficiency of Floating PV systems  
539 compared with Overland PV Systems, Proceedings, The 3rd International Conference on Circuits,  
540 Control, Communication, Electricity, Electronics, Energy, System, Signal and Simulation. pp. 284-289.

541

542 Corripio, J.G., 2019. *insol: Solar Radiation*, 1.2 ed. CRAN.

543

544 Cox, M., 2019. *Floating solar landscape 2019*, Wood Mackenzie Power and Renewables.

545

546 Diehl, S., Berger, S., Ptacnik, R., Wild, A., 2002. Phytoplankton, light, and nutrients in a gradient of  
547 mixing depths: Field experiments. *Ecology* 83(2), 399-411.

548

549 Dörenkämper, M., Wahed, A., Kumar, A., de Jong, M., Kroon, J., Reindl, T., 2021. The cooling effect of  
550 floating PV in two different climate zones: A comparison of field test data from the Netherlands and  
551 Singapore. *Solar Energy* 214, 239-247.

552 Elci, S., 2008. Effects of thermal stratification and mixing on reservoir water quality. *Limnology* 9(2),  
553 135-142.

554

555 Fee, E.J., Hecky, R.E., Kasian, S.E.M., Cruikshank, D.R., 1996. Effects of lake size, water clarity, and  
556 climatic variability on mixing depths in Canadian Shield lakes. *Limnol Oceanogr* 41(5), 912-920.

557

558 Ferrer-Gisbert, C., Ferran-Gozalvez, J.J., Redon-Santafe, M., Ferrer-Gisbert, P., Sanchez-Romero, F.J.,  
559 Torregrosa-Soler, J.B., 2013. A new photovoltaic floating cover system for water reservoirs. *Renew.*  
560 *Energy* 60, 63-70.

561

562 Foley, B., Jones, I.D., Maberly, S.C., Rippey, B., 2012. Long-term changes in oxygen depletion in a  
563 small temperate lake: effects of climate change and eutrophication. *Freshwater Biology* 57(2), 278-  
564 289.

565

566 Ford, D.E., Stefan, H.G., 1980. Thermal Predictions Using Integral Energy-Model. *J Hydr Eng Div-Asce*  
567 106(1), 39-55.

568

569 Forsberg, C., 1989. Importance of Sediments in Understanding Nutrient Cyclings in Lakes.  
570 *Hydrobiologia* 176(1), 263-277.

571

572 Gorjian, S., Sharon, H., Ebadi, H., Kant, K., Scavo, F.B., Tina, G.M., 2021. Recent technical  
573 advancements, economics and environmental impacts of floating photovoltaic solar energy  
574 conversion systems. *Journal of Cleaner Production* 278, 124285.

575

576 Grizzetti, B., Liqueste, C., Pistocchi, A., Vigiak, O., Zulian, G., Bouraoui, F., De Roo, A., Cardoso, A.C.,  
577 2019. Relationship between ecological condition and ecosystem services in European rivers, lakes  
578 and coastal waters. *Sci Total Environ* 671, 452-465.

579

580 Haas, J., Khalighi, J., de la Fuente, A., Gerbersdorf, S.U., Nowak, W., Chen, P.J., 2020. Floating  
581 photovoltaic plants: Ecological impacts versus hydropower operation flexibility. *Energy Conversion*  
582 *and Management* 206, 112414.

583

584 Holm, A., 2017. Floating Solar Photovoltaics Gaining Ground. [https://www.nrel.gov/technical-](https://www.nrel.gov/technical-assistance/blog/posts/floating-solar-photovoltaics-gaining-ground.html)  
585 [assistance/blog/posts/floating-solar-photovoltaics-gaining-ground.html](https://www.nrel.gov/technical-assistance/blog/posts/floating-solar-photovoltaics-gaining-ground.html). (Accessed 09/11/2017  
586 2017).

587

588 Hondzo, M., Stefan, H.G., 1993. Lake Water Temperature Simulation-Model. *Journal of Hydraulic*  
589 *Engineering* 119(11), 1251-1273.

590

591 Huisman, J., van Oostveen, P., Weissing, F.J., 1999. Critical depth and critical turbulence: Two  
592 different mechanisms for the development of phytoplankton blooms. *Limnol Oceanogr* 44(7), 1781-  
593 1787.

594

595 Huisman, J., Sharples, J., Stroom, J.M., Visser, P.M., Kardinaal, W.E.A., Verspagen, J.M.H., Sommeijer,  
596 B., 2004. Changes in turbulent mixing shift competition for light between phytoplankton species.  
597 *Ecology* 85(11), 2960-2970.

598

599 IEA, 2019. 2019 Snapshot of Global PV Markets, Strategic PV Analysis and Outreach.

600

601 Jäger, C.G., Diehl, S., Schmidt, G.M., 2008. Influence of water-column depth and mixing on  
602 phytoplankton biomass, community composition, and nutrients. *Limnol Oceanogr* 53(6), 2361-2373.

603

604 Jesson, D.A., Le Page, B.H., Mulheron, M.J., Smith, P.A., Wallen, A., Cocks, R., Farrow, J., Whiter, J.T.,  
605 2010. Thermally induced strains and stresses in cast iron water distribution pipes: an experimental  
606 investigation. *J Water Supply Res T* 59(4), 221-229.

607

608 Jurvelius, J., Marjomki, T.J., 2008. Night, day, sunrise, sunset: do fish under snow and ice recognize  
609 the difference? *Freshwater Biology* 53(11), ???-???

610

611 Kalff, J., 2002. *Limnology : inland water ecosystems*. Prentice Hall, Upper Saddle River, NJ.

612

613 Knoll, L.B., Sharma, S., Denfeld, B.A., Flaim, G., Hori, Y., Magnuson, J.I., Straile, D., Weyhenmeyer,  
614 G.A., 2019. Consequences of lake and river ice loss on cultural ecosystem services. *Limnol Oceanogr*  
615 *Lett* 4(5), 119-131.

616

617 Kraemer, B.M., Anneville, O., Chandra, S., Dix, M., Kuusisto, E., Livingstone, D.M., Rimmer, A.,  
618 Schladow, S.G., Silow, E., Sitoki, L.M., Tamatamah, R., Vadeboncoeur, Y., McIntyre, P.B., 2015.  
619 Morphometry and average temperature affect lake stratification responses to climate change.  
620 *Geophys. Res. Lett.* 42(12), 4981-4988.

621

622 Kraemer, B.M., Chandra, S., Dell, A.I., Dix, M., Kuusisto, E., Livingstone, D.M., Schladow, S.G., Silow,  
623 E., Sitoki, L.M., Tamatamah, R., McIntyre, P.B., 2017. Global patterns in lake ecosystem responses to  
624 warming based on the temperature dependence of metabolism. *Glob Chang Biol* 23(5), 1881-1890.

625

626 Lee, N., Grunwald, U., Rosenlieb, E., Mirletz, H., Aznar, A., Spencer, R., Cox, S., 2020. Hybrid floating  
627 solar photovoltaics-hydropower systems: Benefits and global assessment of technical potential.  
628 *Renew. Energy* 162, 1415-1427.

629

630 Leppäranta, M., 1993. A review of analytical models of sea-ice growth. *Atmosphere-Ocean* 31(1),  
631 123-138.

632

633 Lerman, A., Imboden, D.M., Gat, J.R., 1995. *Physics and Chemistry of Lakes*. Springer, Berlin.

634

635 Lewis, W.M., 1987. Tropical Limnology. *Annual Review of Ecology and Systematics* 18(1), 159-184.

636

637 Liu, L., Wang, Q., Lin, H., Li, H., Sun, Q., wennifersten, R., 2017. Power Generation Efficiency and  
638 Prospects of Floating Photovoltaic Systems. *Energy Procedia* 105, 1136-1142.

639

640 Livingstone, D.M., Adrian, R., 2009. Modeling the duration of intermittent ice cover on a lake for  
641 climate-change studies. *Limnol Oceanogr* 54(5), 1709-1722.

642

643 Maberly, S.C., Elliott, J.A., 2012. Insights from long-term studies in the Windermere catchment:  
644 external stressors, internal interactions and the structure and function of lake ecosystems.  
645 *Freshwater Biology* 57(2), 233-243.

646

647 Macintyre, S., 1993. Vertical Mixing in a Shallow, Eutrophic Lake - Possible Consequences for the  
648 Light Climate of Phytoplankton. *Limnol Oceanogr* 38(4), 798-817.

649

650 Maestre-Valero, J.F., Martinez-Alvarez, V., Nicolas, E., 2013. Physical, chemical and microbiological  
651 effects of suspended shade cloth covers on stored water for irrigation. *Agricultural Water*  
652 *Management* 118, 70-78.

653

654 Meis, S., Thackeray, S.J., Jones, I.D., 2009. Effects of recent climate change on phytoplankton  
655 phenology in a temperate lake. *Freshwater Biology* 54(9), 1888-1898.

656

657 Maltby, E., Ormerod, S., Acreman, M., Dunbar, M., Jenkins, A., Maberly, S., Newman, J., Blackwell,  
658 M., Ward, R., 2011. *Freshwaters: openwaters, wetlands and floodplains*, UK National Ecosystem  
659 *Assessment: understanding nature's value to society*. UNEP-WCMC, Cambridge, UK, pp. 295-360.

660

661 Moriasi, D.N., Arnold, J.G., Van Liew, M.W., Bingner, R.L., Harmel, R.D., Veith, T.L., 2007. Model  
662 evaluation guidelines for systematic quantification of accuracy in watershed simulations.  
663 *Transactions of the Asabe* 50(3), 885-900.

664

665 Mathijssen, D., Hofs, B., Spiereburg-Sack, E., van Asperen, R., van der Wal, B., Vreeburg, J.,  
666 Ketelaars, H., 2020. Potential impact of floating solar panels on water quality in reservoirs;  
667 pathogens and leaching. *Water Pract Technol* 15(3), 807-811.

668

669 Nash, J.E., Sutcliffe, J.V., 1970. River flow forecasting through conceptual models part I — A  
670 discussion of principles. *J. Hydrol.* 10(3), 282-290.

671

672 National River Flow Archive, 2018. 73010 - Leven at Newby Bridge. National River Flow Archive,  
673 National River Flow Archive.

674

675 North, R.P., North, R.L., Livingstone, D.M., Koster, O., Kipfer, R., 2014. Long-term changes in hypoxia  
676 and soluble reactive phosphorus in the hypolimnion of a large temperate lake: consequences of a  
677 climate regime shift. *Glob Chang Biol* 20(3), 811-823.

678

679 O'Neil, J.M., Davis, T.W., Burford, M.A., Gobler, C.J., 2012. The rise of harmful cyanobacteria blooms:  
680 The potential roles of eutrophication and climate change. *Harmful Algae* 14, 313-334.

681

682 O'Reilly, C.M., Sharma, S., Gray, D.K., Hampton, S.E., Read, J.S., Rowley, R.J., Schneider, P., Lenters,  
683 J.D., McIntyre, P.B., Kraemer, B.M., Weyhenmeyer, G.A., Straile, D., Dong, B., Adrian, R., Allan, M.G.,  
684 Anneville, O., Arvola, L., Austin, J., Bailey, J.L., Baron, J.S., Brookes, J.D., de Eyto, E., Dokulil, M.T.,  
685 Hamilton, D.P., Havens, K., Hetherington, A.L., Higgins, S.N., Hook, S., Izmet'eva, L.R., Joehnk, K.D.,  
686 Kangur, K., Kasprzak, P., Kumagai, M., Kuusisto, E., Leshkevich, G., Livingstone, D.M., MacIntyre, S.,  
687 May, L., Melack, J.M., Mueller-Navarra, D.C., Naumenko, M., Noges, P., Noges, T., North, R.P.,  
688 Plisnier, P.D., Rigos, A., Rimmer, A., Rogora, M., Rudstam, L.G., Rusak, J.A., Salmaso, N., Samal, N.R.,  
689 Schindler, D.E., Schladow, S.G., Schmid, M., Schmidt, S.R., Silow, E., Soyulu, M.E., Teubner, K.,  
690 Verburg, P., Voutilainen, A., Watkinson, A., Williamson, C.E., Zhang, G.Q., 2015. Rapid and highly  
691 variable warming of lake surface waters around the globe. *Geophys. Res. Lett.* 42(24), 10773-10781.

692

693 Oke, T.R., 2002. *Boundary layer climates*. Routledge.

694

695 Oliveira-Pinto, S., Stokkermans, J., 2020. Assessment of the potential of different floating solar  
696 technologies - Overview and analysis of different case studies. *Energy Conversion and Management*  
697 211, 112747.

698

699 Ozkundakci, D., Gsell, A.S., Hintze, T., Tauscher, H., Adrian, R., 2016. Winter severity determines  
700 functional trait composition of phytoplankton in seasonally ice-covered lakes. *Glob Chang Biol* 22(1),  
701 284-298.

702

703 Paerl, H.W., Paul, V.J., 2012. Climate change: links to global expansion of harmful cyanobacteria.  
704 *Water Res* 46(5), 1349-1363.

705

706 Pinto, P.D., Allende, L., O'Farrell, I., 2007. Influence of free-floating plants on the structure of a  
707 natural phytoplankton assemblage: an experimental approach. *Journal of Plankton Research* 29(1),  
708 47-56.

709



710 Ramsbottom, A., 1976. Depth charts of the Cumbrian lakes. Sci. Publ. Freshwater Biol. Assoc.

711

712 Read, J.S., Hamilton, D.P., Desai, A.R., Rose, K.C., MacIntyre, S., Lenters, J.D., Smyth, R.L., Hanson,  
713 P.C., Cole, J.J., Staehr, P.A., Rusak, J.A., Pierson, D.C., Brookes, J.D., Laas, A., Wu, C.H., 2012. Lake-size  
714 dependency of wind shear and convection as controls on gas exchange. *Geophys. Res. Lett.* 39, 5.

715

716 Read, J.S., Hamilton, D.P., Jones, I.D., Muraoka, K., Winslow, L.A., Kroiss, R., Wu, C.H., Gaiser, E.,  
717 2011. Derivation of lake mixing and stratification indices from high-resolution lake buoy data.  
718 *Environmental Modelling & Software* 26(11), 1325-1336.

719

720 Redón-Santafé, M., Ferrer-Gisbert, P.-S., Sánchez-Romero, F.-J., Torregrosa Soler, J.B., Gozalvez, F.,  
721 Javier, J., Ferrer Gisbert, C.M., 2014. Implementation of a photovoltaic floating cover for irrigation  
722 reservoirs. *Journal of cleaner production* 66, 568-570.

723

724 REN21, 2020. *Renewables 2020 Global Status Report*. Paris.

725

726 Reynaud, A., Lanzaova, D., 2017. A Global Meta-Analysis of the Value of Ecosystem Services  
727 Provided by Lakes. *Ecol Econ* 137, 184-194.

728

729 Riley, M.J., Stefan, H.G., 1988. Minlake - a Dynamic Lake Water-Quality Simulation-Model. *Ecological  
730 Modelling* 43(3-4), 155-182.

731

732 Rooney, G.G., Jones, I.D., 2010. Coupling the 1-D lake model FLake to the community land-surface  
733 model JULES. *Boreal Environment Research* 15(5), 501-512.

734

735 Sacramento, E.M.d., Carvalho, P.C.M., de Araújo, J.C., Riffel, D.B., Corrêa, R.M.d.C., Pinheiro Neto,  
736 J.S., 2015. Scenarios for use of floating photovoltaic plants in Brazilian reservoirs. *IET Renewable  
737 Power Generation* 9(8), 1019-1024.

738

739 Sahu, A., Yadav, N., Sudhakar, K., 2016. Floating photovoltaic power plant: A review. *Renew. Sust.  
740 Energ. Rev.* 66, 815-824.

741

742 Saloranta, T.M., 2000. Modeling the evolution of snow, snow ice and ice in the Baltic Sea. *Tellus  
743 Series a-Dynamic Meteorology and Oceanography* 52(1), 93-108.

744

745 Saloranta, T., Andersen, T., 2004. *MyLake v1.1: technical documentation & user's guide*, Norwegian  
746 Institute for Water Research. Norwegian Institute for Water Research.

747

748 Saloranta, T.M., Andersen, T., 2007. MyLake - A multi-year lake simulation model code suitable for  
749 uncertainty and sensitivity analysis simulations. *Ecological Modelling* 207(1), 45-60.

750

751 Santafe, M.R., Gisbert, P.S.F., Romero, F.J.S., Soler, J.B.T., Gozalvez, J.J.F., Gisbert, C.M.F., 2014.  
752 Implementation of a photovoltaic floating cover for irrigation reservoirs. *Journal of Cleaner  
753 Production* 66, 568-570.

754  
755 Solar Asset Management, 2018. TOP 70 FLOATING SOLAR PV PLANTS.  
756 <https://solarassetmanagement.asia/news/top-70-floating-solar-pv-plants>. (Accessed July 2018).  
757  
758 Solarplaza, 2019. A Comprehensive Overview of 200+ Global Floating Solar Plants. pp. 1 - 19.  
759  
760 Stiubiener, U., da Silva, T.C., Trigo, F.B.M., Benedito, R.D., Teixeira, J.C., 2020. PV power generation  
761 on hydro dam's reservoirs in Brazil: A way to improve operational flexibility. *Renew. Energy* 150,  
762 765-776.  
763  
764 Sulaeman, S., Brown, E., Quispe-Abad, R., Muller, N., 2021. Floating PV system as an alternative  
765 pathway to the amazon dam underproduction. *Renew. Sust. Energ. Rev.* 135, 110082.  
766  
767 Taboada, M.E., Caceres, L., Graber, T.A., Galleguillos, H.R., Cabeza, L.F., Rojas, R., 2017. Solar water  
768 heating system and photovoltaic floating cover to reduce evaporation: Experimental results and  
769 modeling. *Renew. Energy* 105, 601-615.  
770  
771 Talling, J.F., 2001. Environmental controls on the functioning of shallow tropical lakes. *Hydrobiologia*  
772 458(1), 1-8.  
773  
774 Thackeray, S.J., Henrys, P.A., Feuchtmayr, H., Jones, I.D., Maberly, S.C., Winfield, I.J., 2013. Food web  
775 de-synchronization in England's largest lake: an assessment based on multiple phenological metrics.  
776 *Glob Chang Biol* 19(12), 3568-3580.  
777  
778 Thackeray, S.J., Jones, I.D., Maberly, S.C., 2008. Long-term change in the phenology of spring  
779 phytoplankton: species-specific responses to nutrient enrichment and climatic change. *Journal of*  
780 *Ecology* 96(3), 523-535.  
781  
782 Tina, G.M., Scavo, F.B., Merlo, L., Bizzarri, F., 2021. Comparative analysis of monofacial and bifacial  
783 photovoltaic modules for floating power plants. *Applied Energy* 281, 116084.  
784  
785 Tranvik, L.J., Downing, J.A., Cotner, J.B., Loiselle, S.A., Striegl, R.G., Ballatore, T.J., Dillon, P., Finlay, K.,  
786 Fortino, K., Knoll, L.B., Kortelainen, P.L., Kutser, T., Larsen, S., Laurion, I., Leech, D.M., McCallister,  
787 S.L., McKnight, D.M., Melack, J.M., Overholt, E., Porter, J.A., Prairie, Y., Renwick, W.H., Roland, F.,  
788 Sherman, B.S., Schindler, D.W., Sobek, S., Tremblay, A., Vanni, M.J., Verschoor, A.M., von  
789 Wachenfeldt, E., Weyhenmeyer, G.A., 2009. Lakes and reservoirs as regulators of carbon cycling and  
790 climate. *Limnol Oceanogr* 54(6), 2298-2314.  
791  
792 Visser, M.E., Both, C., 2005. Shifts in phenology due to global climate change: the need for a  
793 yardstick. *Proc Biol Sci* 272(1581), 2561-2569.  
794  
795 Walsby, A.E., Hayes, P.K., Boje, R., Stal, L.J., 1997. The selective advantage of buoyancy provided by  
796 gas vesicles for planktonic cyanobacteria in the Baltic Sea. *New Phytologist* 136(3), 407-417.  
797

798 Wetzell, R.G., 2001. Limnology: lake and river ecosystems, 3rd ed. Academic Press, San Diego.

799

800 Woolway, R.I., Jones, I.D., Feuchtmayr, H., Maberly, S.C., 2015a. A comparison of the diel variability  
801 in epilimnetic temperature for five lakes in the English Lake District. *Inland Waters* 5(2), 139-154.

802

803 Woolway, R.I., Jones, I.D., Hamilton, D.P., Maberly, S.C., Muraoka, K., Read, J.S., Smyth, R.L.,  
804 Winslow, L.A., 2015b. Automated calculation of surface energy fluxes with high-frequency lake buoy  
805 data. *Environmental Modelling & Software* 70, 191-198.

806

807 Woolway, R.I., Jones, I.D., Maberly, S.C., French, J.R., Livingstone, D.M., Monteith, D.T., Simpson,  
808 G.L., Thackeray, S.J., Andersen, M.R., Battarbee, R.W., DeGasperi, C.L., Evans, C.D., de Eyto, E.,  
809 Feuchtmayr, H., Hamilton, D.P., Kernan, M., Krokowski, J., Rimmer, A., Rose, K.C., Rusak, J.A., Ryves,  
810 D.B., Scott, D.R., Shilland, E.M., Smyth, R.L., Staehr, P.A., Thomas, R., Waldron, S., Weyhenmeyer,  
811 G.A., 2016. Diel Surface Temperature Range Scales with Lake Size. *PLoS One* 11(3), e0152466.

812

813 Woolway, R.I., Meinson, P., Nöges, P., Jones, I.D., Laas, A., 2017. Atmospheric stilling leads to  
814 prolonged thermal stratification in a large shallow polymictic lake. *Climatic Change* 141(4), 759-773.

815

816 Woolway, R.I., Merchant, C.J., 2019. Worldwide alteration of lake mixing regimes in response to  
817 climate change. *Nat. Geosci.* 12(4), 271-+.

818

819 Woolway, R.I., Verburg, P., Lenters, J.D., Merchant, C.J., Hamilton, D.P., Brookes, J., de Eyto, E., Kelly,  
820 S., Healey, N.C., Hook, S., Laas, A., Pierson, D., Rusak, J.A., Kuha, J., Karjalainen, J., Kallio, K., Lepisto,  
821 A., Jones, I.D., 2018. Geographic and temporal variations in turbulent heat loss from lakes: A global  
822 analysis across 45 lakes. *Limnol Oceanogr* 63(6), 2436-2449.

823

824 Woolway, R.I., Verburg, P., Merchant, C.J., Lenters, J.D., Hamilton, D.P., Brookes, J., Kelly, S., Hook,  
825 S., Laas, A., Pierson, D., Rimmer, A., Rusak, J.A., Jones, I.D., 2017. Latitude and lake size are  
826 important predictors of over-lake atmospheric stability. *Geophys. Res. Lett.* 44(17), 8875-8883.

827

828 Woolway, R.I., Weyhenmeyer, G.A., Schmid, M., Dokulil, M.T., de Eyto, E., Maberly, S.C., May, L.,  
829 Merchant, C.J., 2019. Substantial increase in minimum lake surface temperatures under climate  
830 change. *Climatic Change* 155(1), 81-94.

831

832 World Bank Group, ESMAP, SERIS, 2018. Where Sun Meets Water : Floating Solar Market Report.  
833 Washington, D.C.

834

835 World Bank Group, ESMAP, SERIS, 2019. Where Sun Meets Water: Floating Solar Handbook for  
836 Practitioners. Washington, DC.

837

838 Yadav, N., Gupta, M., Sudhakar, K., Ieee, 2016. Energy Assessment of Floating Photovoltaic System.

839

840 Yankova, Y., Neuenschwander, S., Koster, O., Posch, T., 2017. Abrupt stop of deep water turnover  
841 with lake warming: Drastic consequences for algal primary producers. *Sci Rep* 7(1), 13770.

- 842  
843 Zhang, N., Jiang, T., Guo, C., Qiao, L.F., Ji, Q., Yin, L.Q., Yu, L.M., Murto, P., Xu, X.F., 2020. High-  
844 performance semitransparent polymer solar cells floating on water: Rational analysis of power  
845 generation, water evaporation and algal growth. *Nano Energy* 77, 105111.
- 846  
847 Zhou, Y.L., Chang, F.J., Chang, L.C., Lee, W.D., Huang, A., Xu, C.Y., Guo, S.L., 2020. An advanced  
848 complementary scheme of floating photovoltaic and hydropower generation flourishing water-food-  
849 energy nexus synergies. *Applied Energy* 275, 115389.
- 850  
851 Ziar, H., Prudon, B., Lin, F.Y., Roeffen, B., Heijkoop, D., Stark, T., Teurlincx, S., Domis, L.D., Goma, E.G.,  
852 Extebarria, J.G., Alavez, I.N., van Tilborg, D., van Laar, H., Santbergen, R., Isabella, O., 2020.  
853 Innovative floating bifacial photovoltaic solutions for inland water areas. *Prog Photovoltaics*.